

# Theory of Spin Orientation of Semiconductor Carriers at a Ferromagnetic Interface

J. P. McGuire, C. Ciuti, and L. J. Sham

*Department of Physics, University of California San Diego, La Jolla CA 92093-0319.*

(Dated: November 13, 2018)

A quantum theory of the spin-dependent scattering of semiconductor electrons by a Schottky barrier at an interface with a ferromagnet is presented. The reflection of unpolarized non-equilibrium carriers produces spontaneous spin-polarization in the semiconductor. If a net spin-polarization pre-exists in the semiconductor, the combination of the ferromagnet magnetization and the incident carrier polarization combine to tilt the reflected polarization in the semiconductor. The spin reflection properties are investigated as functions of the system characteristics: the Schottky barrier height, semiconductor doping and applied bias. The effect on reflection due to the variation of the barrier width with electron energy is contrasted for two means of excitation: optical or electrical. Optically excited electrons have a wider energy spread than the near-equilibrium excitation from non-magnetic ohmic contacts.

## I. INTRODUCTION

Semiconductor spintronics<sup>1</sup> is a new field in which the manipulation of carrier spins is a central issue. The first device proposal in this field was by Datta and Das,<sup>2</sup> which consisted of (1) spin injection from a ferromagnet source contact into a semiconductor two-dimensional electron gas (2DEG), (2) manipulation of the spin with a gate bias through the Rashba spin-orbit effect,<sup>3</sup> and (3) measurement of the spin with a ferromagnetic drain contact. Progress has recently been made both in spin injection<sup>4,5,6,7,8</sup> and in control via the Rashba effect<sup>9</sup> but it appears that there are difficulties in practical implementation of this kind of device. The demand of sufficiently strong spin-orbit interaction requires a narrow gap semiconductor. More basically, the spin-orbit interaction driven by the electric field normal to the plane of the electron gas polarizes the electron spin in the plane normal to its wave vector. To reduce spin-cancellation effects among different wave-vectors,<sup>10</sup> a one-dimensional channel was suggested.<sup>2</sup> In this paper, we describe in theory a different approach to generate and control spin polarization in semiconductors which is based on the spin-dependent properties of thin semiconductor layers in close proximity to a ferromagnet.

Time-resolved Faraday rotation experiments over the last decade have given much insight into electron spin dynamics in semiconductors.<sup>11</sup> In particular, it has been shown that in lightly doped semiconductors the electron spin coherence can persist for hundreds of nanoseconds,<sup>12</sup> a packet of spin-coherent electrons can be dragged microns using an electrical bias<sup>13</sup> and can maintain their coherence through an interface between two semiconductors,<sup>14</sup> and electron spin coherence can produce large nuclear effects<sup>15</sup> in the semiconductor through the hyperfine interaction<sup>16</sup>. Recent pump-probe experiments have been performed on *n*-doped semiconductor epilayers in contact with a ferromagnet, demonstrating that the proximity of the ferromagnet can induce large nuclear fields<sup>17</sup> and spontaneous electron spin polarization<sup>18</sup> in the semiconductor. In a recent letter,<sup>19</sup> we gave a theory of spin-dependent reflection at the

semiconductor-ferromagnet Schottky barrier as an explanation of the origin of the spin polarization. In this long paper, we provide a detailed treatment of the spin reflection. We also include calculated results of applying electric bias between the semiconductor and the ferromagnet, stimulated by an ongoing experiment under bias.<sup>20</sup> We also investigate the different spin reflection properties resulting from optical pumping and from electrical excitation of non-equilibrium carriers in the semiconductor.

The paper is organized as follows. Section II gives a description of the physics of semiconductor electron spin polarization upon reflection at a semiconductor-ferromagnet interface. In Section III we present the general scattering theory. In Section IV, we apply the theory to the case of Schottky junction, showing the role of the Schottky barrier, semiconductor doping and applied bias. Moreover, we compare the case of optical excitation to that of electrical excitation. Conclusions are drawn in Section V.

## II. SPIN REFLECTION OFF A FERROMAGNET

The generation of spin polarization by scattering of spin particles against a spin-polarized target has a long history.<sup>21</sup> We consider the situation where a non-equilibrium distribution of carriers is injected in the semiconductor (either electrically or optically) and determine the transient spin-dependent reflection dynamics. The semiconductor is assumed to be *n*-doped to ensure a reasonably thin Schottky barrier (for sizeable quantum-mechanical coupling between the semiconductor and the ferromagnet) and reduced spin relaxation. Thus, an initially spin-compensated group of excited electrons will be reflected by the ferromagnetic interface with a net spin polarization. Since the momentum relaxation of the non-equilibrium carriers is much faster than their spin relaxation, the Fermi sea in the semiconductor conduction band is left with a spin polarization. In this way, the spin reflection produces a ferromagnetic “imprinting” of the semiconductor electrons. More generally, if the non-

equilibrium electrons have a pre-existing spin polarization, the ferromagnetic imprinting manifests itself as a tilting of the original polarization vector. Thus, the spin reflection not only generates a spin polarization, but can also rotate a pre-existing ensemble spin.

In the case of optical excitation one should also consider the spin dynamics of the excited holes in the valence band. However, we will neglect any spin effects from the valence band holes. The holes can gain polarization from the reflection at the interface exactly as the conduction electrons, but the corresponding spin polarization is known to decay very fast due to valence band-mixing.<sup>22</sup> In particular the hole spin relaxation time is much shorter than the optical electron-hole recombination time. In the case of optical excitation, a moderate electron doping is essential to provide very long spin lifetimes<sup>12</sup>, because the Fermi sea acts as a spin reservoir. The holes will recombine with electrons from the Fermi sea and thus remove a strong source of electron relaxation via exchange with the holes.<sup>23</sup>

### III. THEORY OF SPIN-DEPENDENT REFLECTION

To capture the essential physics of the problem we work with a simplified effective mass Hamiltonian in both the semiconductor and the ferromagnet.<sup>24</sup> The effective mass approximation, though suitable for semiconductor heterostructures, can not possibly account for all band properties of the ferromagnetic metal.<sup>25</sup> We shall investigate one improvement of the wave function matching between the dissimilar metal and semiconductor media.<sup>26</sup> The general results we present should remain valid with more realistic calculations.

The Hamiltonian of the metal/semiconductor junction is given by

$$H = -\frac{\hbar^2}{2} \frac{d}{dz} \left[ \frac{1}{m^*(z)} \frac{d}{dz} \right] + U(z) + \frac{\Delta}{2} \boldsymbol{\sigma} \cdot \hat{\mathbf{M}} \Theta(z) + \frac{g^*}{2} \mu_B \boldsymbol{\sigma} \cdot \mathbf{B}_{\text{tot}} \Theta(-z), \quad (1)$$

where the  $z$ -axis is along the growth direction. The first term is the kinetic energy, where  $m^*(z)$  is the effective mass which is different for each region. The second term represents the spin-independent part of the potential energy. In the semiconductor region ( $z < 0$ ), the potential  $U(z)$  produces the band-bending due to the space charge layer associated with the Schottky barrier.  $U(z)$  can be tailored by proper heterostructure engineering (for example by inserting a delta-doped layer at the interface) or by applying *in situ* an electrostatic bias. As we will show in detail in Section IV, the profile of  $U(z)$  can drastically modify the spin-dependent coupling between semiconductor and ferromagnet. The second line of Eq. (1) contains the spin-dependent part of the Hamiltonian, the exchange interaction operator in the ferromagnet ( $z > 0$ )

and the Zeeman energy in the semiconductor ( $z < 0$ ).  $\Delta$  is the exchange splitting energy between the majority and minority spin bands in the ferromagnet and  $\hat{\mathbf{M}}$  is the unit vector along the direction of the ferromagnet magnetization. In the Zeeman term,  $g^*$  is the effective electron g-factor ( $g^* = -0.44$  for GaAs),  $\mu_B$  is the Bohr magneton, and the magnetic field  $\mathbf{B}_{\text{tot}}$  is the sum of the external field and the induced nuclear field,  $\mathbf{B}_{\text{tot}} = \mathbf{B} + \mathbf{B}_N$ . The Zeeman splitting has a negligible effect on the spin polarization because it is typically several orders of magnitude smaller than the exchange splitting in the ferromagnet and the Schottky barrier height. However, a weak magnetic field is useful as a probe of the ferromagnetic imprinting, because it induces a Larmor precession of the reflection-induced spin polarization which can be detected, for example, by time-resolved Faraday rotation.<sup>17</sup> The origin of the nuclear field  $\mathbf{B}_N$  is the hyperfine coupling between the electron and the nuclear spins. If the electron polarization has a component along the external magnetic field vector, the electron polarization is known to induce dynamically a nuclear spin polarization through the Overhauser effect.<sup>17</sup> The dynamically polarized nuclei produce an effective magnetic field that acts back on the electrons

$$\mathbf{B}_N \sim \frac{g^*}{|g^*|} \frac{(\mathbf{S} \cdot \mathbf{B}) \mathbf{B}}{B^2 + B_0^2}. \quad (2)$$

Depending on the orientation of the electron spin polarization vector  $\mathbf{S}$  relative to  $\mathbf{B}$ , the nuclei can align either along or against the external applied field.  $B_0$  is a phenomenological parameter to account for the fact that at low applied field the nuclei are unable to align with the applied field due to nuclear spin-spin interactions which tend to destroy the dynamic nuclear polarization.

We denote a majority spin in the ferromagnet as  $|+\rangle$  and a minority spin in the ferromagnet as  $|-\rangle$ , which are eigenstates of the exchange splitting operator,  $\boldsymbol{\sigma} \cdot \hat{\mathbf{M}} |\pm\rangle = \mp |\pm\rangle$  (the magnetization is antiparallel to the net electron spin). In the following, we will work explicitly in this basis. In general, the reflection of semiconductor electrons at the ferromagnetic interface is represented by the reflection matrix  $\hat{r}(\mathbf{k})$ , which, in the ferromagnet spin basis, is

$$\hat{r}(\mathbf{k}) = \begin{pmatrix} r_{+,\mathbf{k}} & 0 \\ 0 & r_{-,\mathbf{k}} \end{pmatrix}, \quad (3)$$

where  $r_{+,\mathbf{k}}$  is the reflection coefficient for a semiconductor electron with its spin aligned with the majority spin band in the ferromagnet and  $r_{-,\mathbf{k}}$  likewise with the minority spin band. This can be expressed in the vectorial form

$$\hat{r}(\mathbf{k}) = \frac{1}{2} \left[ (r_{-,\mathbf{k}} + r_{+,\mathbf{k}}) \mathbb{1} + (r_{-,\mathbf{k}} - r_{+,\mathbf{k}}) \hat{\mathbf{M}} \cdot \boldsymbol{\sigma} \right], \quad (4)$$

where  $\mathbb{1}$  is the unit matrix.

Suppose that a short excitation pulse injects non-equilibrium electrons into the semiconductor. This perturbation can be applied either by a short optical pump

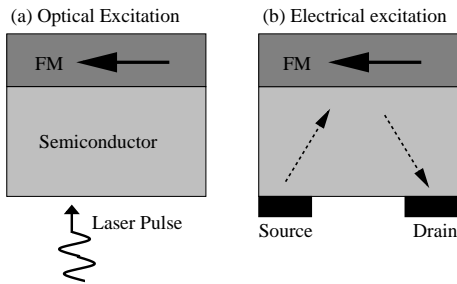


FIG. 1: The excitation of non-equilibrium electrons into a semiconductor. In (a), a short laser pulse with energy at or above the bandgap of the semiconductor creates a distribution of electrons related to the laser spectrum. In (b), a source contact or an STM tip can inject electrons at or above the Fermi level in the semiconductor. In both cases the non-equilibrium electrons can reflect off the interface with a ferromagnet.

pulse or electrically through lateral contacts or an STM tip (see Fig. 1). Initially, the non-equilibrium electron spin density matrix has the form

$$\hat{\rho}^i(\mathbf{k}, t=0) = \frac{1}{2} f^i(k) (\mathbb{1} + \mathbf{P}^i \cdot \boldsymbol{\sigma}), \quad (5)$$

with  $f^i(k)$  the distribution of injected electrons (for optical excitation it depends on the laser spectrum). The initial polarization is determined by the perturbation. Optically, the polarization is determined by the usual selection rules, namely  $\mathbf{P}^i = 0$  for linearly polarized light and  $\mathbf{P}^i \neq 0$  for elliptically polarized light. In the case of electrical excitation, an initial polarization can be created through injection from magnetic contacts through ordinary spin injection. Upon striking the interface, the non-equilibrium electrons will reflect and transmit, and, to fully account for the polarization in the semiconductor, we must calculate the effect of this reflection on the spin density matrix:

$$\begin{aligned} \hat{\rho}^r(\mathbf{k}, t) &= \hat{r}(\mathbf{k}) \hat{\rho}^i(\mathbf{k}, t) \hat{r}^\dagger(\mathbf{k}) \\ &= f^i(k, t) \frac{1}{2} [R_0(\mathbf{k}) \mathbb{1} + \mathbf{R}(\mathbf{k}) \cdot \boldsymbol{\sigma}], \end{aligned} \quad (6)$$

where, with the  $\mathbf{k}$ -dependence understood,

$$\begin{aligned} R_0 &= \frac{1}{2} [(|r_-|^2 + |r_+|^2) + (|r_-|^2 - |r_+|^2) \hat{\mathbf{M}} \cdot \mathbf{P}^i], \quad (7) \\ \mathbf{R} &= \frac{1}{2} [(|r_-|^2 - |r_+|^2) + (|r_-|^2 + |r_+|^2) \hat{\mathbf{M}} \cdot \mathbf{P}^i] \hat{\mathbf{M}} \\ &\quad + \text{Re}(r_- r_+^*) (\hat{\mathbf{M}} \times \mathbf{P}^i) \times \hat{\mathbf{M}} - \text{Im}(r_- r_+^*) \hat{\mathbf{M}} \times \mathbf{P}^i. \end{aligned} \quad (8)$$

In general the polarization after reflection  $\mathbf{R}(\mathbf{k})$  is different from the original polarization  $\mathbf{P}^i$  of the excited electrons in the semiconductor.

Since the electron distribution is not in equilibrium, the relaxation of the spin density matrix will be dominated by the relaxation of the hot carrier distribution,  $f^i(k, t) = f^i(k) \exp(-t/\tau_k)$ . This relaxation

is spin-independent because it occurs on a much faster time scale than the spin-relaxation time. Thus, the reflection-induced spin-polarization will leave a spin excitation in the semiconductor electron sea. In order to quantitatively determine the effect, we need to calculate the current flow into the ferromagnet during the non-equilibrium transient,

$$\hat{j}(t) = \hat{j}^i(t) + \hat{j}^r(t) = \int_{k_z > 0} \frac{d^3 \mathbf{k}}{(2\pi)^3} [\hat{\rho}^i(\mathbf{k}, t) - \hat{\rho}^r(\mathbf{k}, t)] v_z, \quad (9)$$

where  $v_z = \hbar k_z / m_{\text{sc}}^*$  is the velocity component normal to the interface. This current flow will be spin-dependent, so that the net spin in the semiconductor from the reflection will be the negative of the spin transmitted into the ferromagnet,

$$\begin{aligned} \mathbf{S}^r &= -\text{Tr} \left\{ \frac{\hbar}{2} \boldsymbol{\sigma} \int dt [\hat{j}^i(t) + \hat{j}^r(t)] \right\} \\ &= \frac{\hbar}{2} \int_{k_z > 0} \frac{d^3 \mathbf{k}}{(2\pi)^3} f^i(k) [\mathbf{R}(\mathbf{k}) - \mathbf{P}^i] \tau_k v_z. \end{aligned} \quad (10)$$

This is the spin density per unit area, so that the total spin density per unit area in the semiconductor after reflection is

$$\mathbf{S} = n^i \frac{\hbar}{2} \mathbf{P}^i L + \mathbf{S}^r, \quad (11)$$

where  $n^i = \int \frac{d^3 \mathbf{k}}{(2\pi)^3} f^i(k)$  is the volume density of pumped electrons and  $L$  is the semiconductor length perpendicular to the interface. As shown in Eq. (10), the contribution to the imprinted spin from each wavevector channel is proportional to the mean-free path  $\tau_k v_z$ . Only the fraction of non-equilibrium electrons within a mean-free path of the interface participate in the spin-dependent reflection. This implies that for increasing sample length  $L$ , the imprinted spin density per unit volume decreases as  $1/L$ . In the opposite limit, with the semiconductor length  $L$  shorter than the mean-free path, the situation is different because multiple reflections occur and the electrons are quantum confined. This was the impetus behind a recent proposal for a spin valve with ferromagnetic gates<sup>30</sup> and will be addressed in a future publication.

After the non-equilibrium transient, the imprinted spin of the semiconductor electron sea will decay with the long spin relaxation time. A weak magnetic field induces a Larmor precession which is useful for measuring the imprinted spin. The evolution of the spin in the semiconductor is governed by the Bloch equation

$$\frac{d\mathbf{S}}{dt} = \frac{g^* \mu_B}{\hbar} \mathbf{B}_{\text{tot}} \times \mathbf{S}(t) - \frac{\mathbf{S}(t)}{T_2^*}. \quad (12)$$

The component of  $\mathbf{S}$  orthogonal to the applied field  $\mathbf{B}$  can be extracted from the amplitude of the Larmor precession. In addition, by measuring the effective Larmor frequency it is possible to extract the nuclear field  $\mathbf{B}_N$  (which is proportional to the component of  $\mathbf{S}$  along the

magnetic field). There are three basic vectors in the problem that determine the Faraday rotation: the external field  $\mathbf{B}$ , the ferromagnet magnetization  $\mathbf{M}$ , and the injected pump polarization  $\mathbf{P}^i$ . Our theory can be tested by systematically changing the relative orientations of these vectors. We now discuss separately the cases of unpolarized and polarized excitation.

### A. Unpolarized Excitation

The excited electron population is unpolarized,  $\mathbf{P}^i = 0$ , when the non-equilibrium electrons are injected by a linearly polarized laser or a non-magnetic electrical contact. Although initially unpolarized, the non-equilibrium electrons will be polarized by the reflection process. This can be understood in simple terms. Since the majority and minority spin electrons have different wavevectors in the ferromagnet (i.e., the two spin bands are exchange split), the reflection coefficients will in general be different for the two spin channels. This will leave a net *spontaneous* polarization in the semiconductor.

The polarization process by spin-reflection for unpolarized excitation from a pump beam is shown in Fig. 2 using a simplified model of a parabolic conduction band and a single parabolic valence band. (a) The semiconductor is lightly *n*-doped to maximize the spin lifetime, so there is an unpolarized background Fermi sea of electrons. (b) A linearly polarized pump beam excites spin-compensated non-equilibrium electrons and holes. The electrons reflect off the interface. The different reflection coefficients of the two spin channels create a net spin polarization in the semiconductor. The holes undergo a similar process, but the spin-orbit coupling rapidly relaxes any polarization in the valence band. (c) Energy and momentum relaxation then drives the electrons and holes to the lowest available states, with a net spin polarization remaining in the conduction band. (d) After the electron-hole recombination time, all excess holes are gone, and a net polarization is left in the Fermi sea of the conduction band. (e) After the long spin-relaxation time, the electron Fermi sea relaxes back to its original unpolarized state.

The spin in the semiconductor after reflection will be

$$\mathbf{S}^r = \frac{\hbar}{4} \hat{\mathbf{M}} \int_{k_z > 0} \frac{d^3 \mathbf{k}}{(2\pi)^3} f^i(k) (|r_{-, \mathbf{k}}|^2 - |r_{+, \mathbf{k}}|^2) \tau_k v_z, \quad (13)$$

and hence is determined by the difference in the spin-dependent reflectivities. The spin asymmetry is quantum mechanical in origin, so the sign of the polarization can be positive or negative. The coupling between the ferromagnet and semiconductor is more efficient for either the majority or minority electrons depending on the electronic structure of the ferromagnet and the form of the interface potential in the semiconductor. The spontaneous spin polarization is thus either parallel or antiparallel to the ferromagnet magnetization  $\mathbf{M}$ .

Our theory offers a possible explanation of the findings of the recent time-resolved Faraday experiments by Epstein *et al.*<sup>18</sup> After pumping non-equilibrium unpolarized electrons in the semiconductor, the experiment found that the system quickly acquired (in tens of picoseconds, consistent with the orbital relaxation time) a spontaneous spin polarization which then decayed with the long spin relaxation time (nanoseconds). The imprinted spin  $\mathbf{S}^r$  was aligned along  $\mathbf{M}$  by varying the angle between the applied field  $\mathbf{B}$  and the magnetization  $\mathbf{M}$ . Interestingly, different ferromagnetic materials gave different signs of the spin polarization relative to  $\mathbf{M}$ .

### B. Polarized Excitation

When the electrons are pumped with a net polarization  $\mathbf{P}^i \neq 0$ , the reflected spin does not align with  $\mathbf{M}$  or  $\mathbf{P}^i$ . There is an extra component which is perpendicular both to  $\mathbf{M}$  and  $\mathbf{P}^i$ , i.e., the reflection off the ferromagnet produces a spin-torque. The geometry of the process is depicted in Fig. 3(a). The amplitude of the extra component is proportional to  $\text{Im}(r_- r_+^*)$ , implying that the spin torque is due to the different reflection phase-shift for minority and majority spin channels. A pre-existing spin polarization vector can be manipulated using this property of the reflection process, as is shown schematically in Fig. 3(b).

In principle, this kind of effect can be detected through time-resolved Faraday rotation experiments with circularly polarized light. Tilting of the optically injected polarization vector due to reflection would appear as a phase-shift in the Larmor precession. The spin torque term, which is aligned along  $\mathbf{M} \times \mathbf{P}^i$ , would change sign if the magnetization were switched,  $\mathbf{M} \rightarrow -\mathbf{M}$ , resulting in a jump in the phase of the Larmor precession. Experimental studies of this phase shift have been observed. However, a systematic study as a function of the relative geometric orientation of optically-injected polarization, ferromagnet magnetization and magnetic field are necessary to fully test our theoretical predictions.

The *spin torque* term we describe is analogous to an effect predicted by Slonczewski<sup>27</sup> and recently demonstrated in all-metallic systems.<sup>28</sup> A spin-polarized current injected into a ferromagnet can tilt the magnetization of the ferromagnet, provided that (1) the ferromagnet magnetization and the polarization of the current are not collinear, and (2) the spin-polarized current injected into the ferromagnet is quite large. However, in the system that we consider, the density of carriers in the semiconductor is so small compared to the density of carriers in the ferromagnet that the tilting of the ferromagnet magnetization is negligible. Instead we find complementary behavior in which the ferromagnet magnetization tilts the polarization of the current.

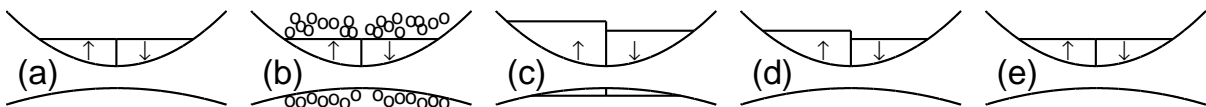


FIG. 2: The polarization process by spin-reflection for unpolarized excitation by a pump beam. Explanation is in the text.

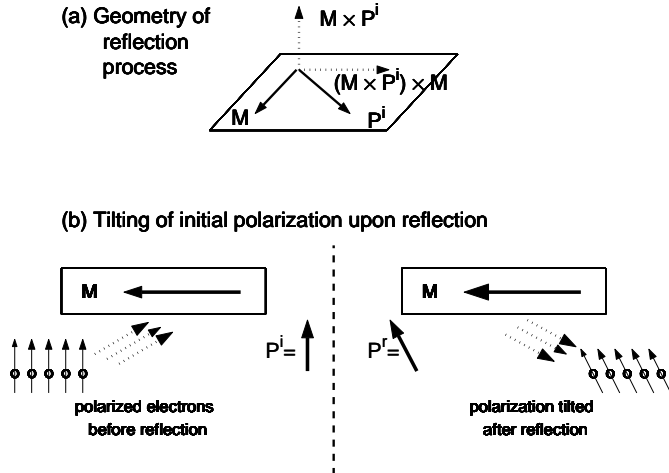


FIG. 3: (a) The geometry of the reflection process for polarized excitation. In general, the reflected polarization has components along all three spatial directions. (b) A net spin polarization present before reflection will be tilted upon the interaction at the interface.

#### IV. RESULTS FOR A SCHOTTKY BARRIER

In this section we investigate in detail the spin reflection at the Schottky barrier between a homogeneously  $n$ -doped semiconductor and a ferromagnetic metal. We define the zero of the potential energy at the Fermi level in the metal. Within the depletion layer approximation, the potential energy in the semiconductor space-charge region ( $-z_b < z < 0$ ) is given by

$$U(x) = V - E_f^{\text{sc}} + (U_b + E_f^{\text{sc}} - V) \left(1 + \frac{z}{z_b}\right)^2, \quad (14)$$

where  $V$  is the applied bias,  $E_f^{\text{sc}}$  is the Fermi kinetic energy in the semiconductor,  $U_b$  is the Schottky barrier height, and  $z_b = \sqrt{\epsilon_0 U_b / (2\pi n e^2)}$  is the depletion width. For high bias  $V > U_b + E_f^{\text{sc}}$ , the semiconductor is considered at flat band. The depletion approximation could be replaced with a more realistic model, such as one constructed using the coupled Poisson and Thomas-Fermi equations, but we have explicitly calculated and verified that the deviation from the depletion approximation is negligible.

In Ref. 19 we gave an analytical approximation for the spin-dependent reflection using an effective rectangular barrier. In this paper, we show the exact numerical results for the realistic Schottky potential in Eq. (14).

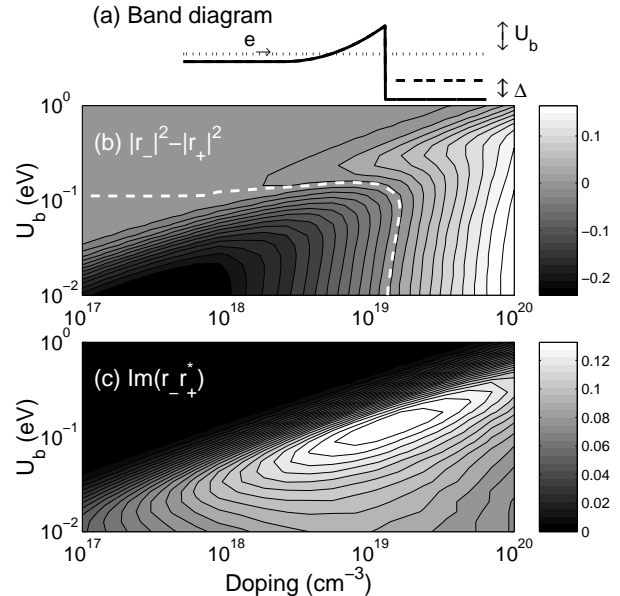


FIG. 4: Reflection from the Schottky junction in equilibrium. (a) The band diagram for the calculation. The electrons are incident from the Fermi level in the semiconductor. (b) Contours of the spin reflection asymmetry  $|r_-|^2 - |r_+|^2$  as a function of the semiconductor doping  $n$  and the Schottky barrier height  $U_b$ . This quantity changes sign at the white dashed line. (c) The component of reflected polarization orthogonal to both  $\mathbf{M}$  and  $\mathbf{P}^i$ , which is always positive.

We also present results for the optical excitation of non-equilibrium electrons, in which pumping takes place in the barrier region, and contrast them with the results for excitation at the Fermi level (electrical injection). These are of interest since both transport and optical experiments have been performed on Schottky barriers in which spin reflection plays a role.

##### A. Unbiased Schottky barrier

Under no applied bias,  $V = 0$ , the semiconductor and the ferromagnet are in equilibrium, so that the Fermi levels in the two systems are equal. We consider the spin-dependent reflection of electrons which are incident on the Schottky barrier from the semiconductor side with the Fermi kinetic energy  $E_f^{\text{sc}} = \hbar^2 (3\pi^2 n)^{2/3} / (2m_{\text{sc}}^*)$ . The spin-dependence of the reflection coefficient arises from the spin-dependent Fermi velocities in the ferromagnet, which are, in the two-band model,  $v_+^{\text{fm}} = \sqrt{2E_f^{\text{fm}} / m_{\text{fm}}^*}$

and  $v_-^{\text{fm}} = \sqrt{2(E_f^{\text{fm}} - \Delta)/m_{\text{fm}}^*}$  for the majority and minority spin, respectively.  $E_f^{\text{fm}}$  and  $m_{\text{fm}}^*$  are the Fermi energy and effective mass in the ferromagnet.

The numerical results for the reflection coefficients have been obtained through a finite-difference solution of the Schrödinger equation.<sup>29</sup> The input parameters for the semiconductor are those of bulk GaAs ( $m_{\text{sc}}^* = 0.07 m_0$ ,  $\epsilon = 12.9$ ). For the ferromagnet, we use the values  $m_{\text{fm}}^* = 1$ ,  $E_f^{\text{fm}} = 2.5$  eV,  $\Delta = 1.9$  eV). We show the results for the spin reflection difference  $|r_-|^2 - |r_+|^2$  and the spin torque amplitude  $\text{Im}(r_-^* r_+)$  as functions of the semiconductor doping  $n$  and Schottky barrier height  $U_b$  are shown in Fig. 4.

Fig. 4(b) shows the spin difference  $|r_-|^2 - |r_+|^2$ , which is the spin polarization generated by reflection, directed along the ferromagnet magnetization,  $\mathbf{M}$ . Both the Schottky barrier height and the semiconductor doping have significant impact on this generated spin polarization. Variation of either property within experimentally accessible values can cause a change of direction of the spin polarization (indicated by the white-dashed line). The numerical results for the realistic Schottky potential show that our approximated solutions with an effective rectangular barrier in Ref. 19 are very close. The shape of the contours are identical and only minor discrepancies are present. Note that, even in the absence of a barrier, the velocity mismatch at the interface leads to spin-dependent reflection. At low doping  $n < 10^{19} \text{cm}^{-3}$ , the semiconductor velocity is better matched to the minority spin band velocity, but at high doping  $n > 10^{19} \text{cm}^{-3}$ , the semiconductor velocity is better matched to the majority spin band velocity (since the Fermi energy for minority spins is smaller than the Fermi energy for majority spins). This is the reason for a change of sign in the spin difference as a function of doping. This argument may be extended to interfaces with small Schottky barriers, but for large Schottky barriers tunneling plays a dominant role. Fig. 4(b) shows the sign change of the spin difference when the barrier height is larger than about 0.1 eV that joins smoothly with the change of sign from the low-barrier region. For large Schottky barriers, the large wave-vector in the barrier region better matches the majority spin band velocity, inducing the change of sign.

Figure 4(c) shows the spin torque term for polarized incident electrons. This is the reflected polarization component orthogonal to both the ferromagnet magnetization  $\mathbf{M}$  and the electron polarization  $\mathbf{P}^i$ . We find that this term always has the same sign and is analogous to the Kramers-Kronig partner of the spin difference shown in Fig. 4(b).

In the effective mass model used above for both the metal and the semiconductor, we match the wave function and its derivative with the only accommodation of the effect the different crystals being the effective masses ( $\psi'/m^*$  is continuous). We have investigated the effect of the semiconductor band structure effect in the limit of small gap with the boundary condition<sup>26</sup> which modifies the envelope wave function slope on the semi-

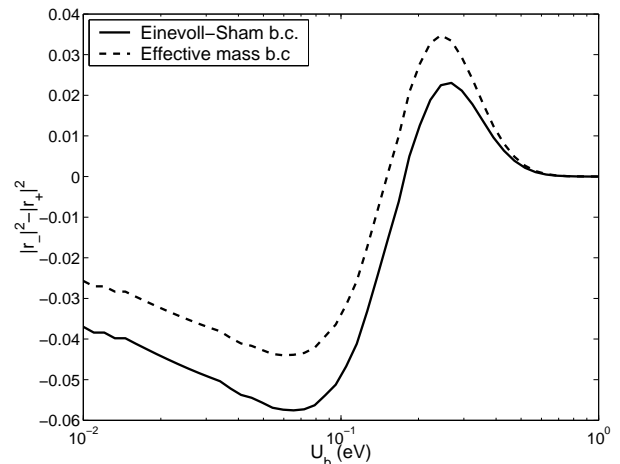


FIG. 5: A comparison of the spin reflection asymmetry using the effective mass boundary condition and the Einevoll-Sham<sup>26</sup> boundary condition. The semiconductor density is fixed at  $n = 10^{19} \text{cm}^{-3}$ .

conductor side by a factor of a half,

$$\frac{1}{2m_{\text{sc}}^*} \frac{\psi'_{\text{sc}}}{\psi_{\text{sc}}} = \frac{1}{m_{\text{fm}}^*} \frac{\psi'_{\text{fm}}}{\psi_{\text{fm}}}. \quad (15)$$

We have found that the spin property dependence on the barrier height and doping density qualitatively unchanged (see Fig. 5).

Our theory implies that the reflected spin polarization is very dependent on the band profile in the semiconductor. The Schottky barrier height  $U_b$  and barrier width as measured by the semiconductor doping  $n$  have a large impact on both the sign and magnitude of the polarization. Both effects can be used to *tailor* the Schottky barrier to achieve the desired spin polarization through different ferromagnetic materials and different doping concentrations. Our results also show that spin polarization generation through the transmission or reflection of a barrier is a quantum mechanical phenomenon. As is evident from our plot, the reflection can not simply be modelled as depending on the ferromagnetic density of states, or as a spin-dependent resistance that is insensitive to the exact properties of the barrier.

## B. The effect of an applied bias

Now we examine the effect of applying a bias across the Schottky barrier. We assume that applying a positive bias  $V > 0$  raises the semiconductor Fermi level above the ferromagnet Fermi level by an amount  $V$ , i.e., the entire voltage drop is across the barrier; the semiconductor bulk and the ferromagnet bulk are assumed to be flat. The bias may be viewed approximately as just changing the Schottky barrier height, so that for negative bias the Schottky barrier is larger by  $V$  and for positive bias the Schottky barrier is smaller by  $V$ . For  $V > (U_b + E_f^{\text{sc}})$ , the

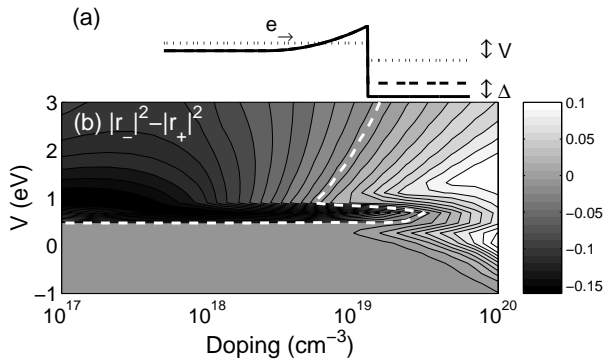


FIG. 6: Reflection from the biased Schottky barrier. (a) The band diagram. For negative bias, the semiconductor Fermi level is below the ferromagnet Fermi level. For  $V > (U_b + E_f^{\text{sc}})$  the semiconductor is in flat band condition and the electrons see no barrier. The Schottky barrier height is fixed at  $U_b = 0.7 \text{ eV}$ . (b) The spin reflection asymmetry as a function of semiconductor doping  $n$  and applied bias  $V$ . The change of sign is indicated by the dashed white line, and its horizontal segment is near the Schottky barrier height.

barrier disappears and the entire semiconductor region is a flat band. Moreover, since the tunnelling is a ballistic process, the bias implies that the transmission into the ferromagnet is not at the Fermi level in the ferromagnet. Thus the applied bias changes the majority and minority velocities and hence the matching of the semiconductor electrons (at the Fermi level in the semiconductor  $E_f^{\text{sc}}$ ). In this calculation we choose the Schottky barrier height to be  $U_b = 0.7 \text{ eV}$ , the value of Fe/GaAs.

In Fig. 6 we plot the spin reflection difference  $|r_-|^2 - |r_+|^2$  for unpolarized excitation. At  $V = 0$ , this corresponds to a slice out of Fig. 4 at the Schottky barrier height  $U_b = 0.7 \text{ eV}$ . As the figure shows, changing the bias makes a change of sign in the spin reflection difference in a similar way to the change of sign as a function of Schottky barrier height in Fig. 4(b). For negative bias  $V < 0$ , the Schottky barrier increases in both height and width. The net effect is that the reflection coefficients for both spin channels are very nearly unity, so that the difference between them is negligible. The sign of the polarization is the same as the sign at zero bias, but the spin difference goes asymptotically to zero. The sign of the polarization changes abruptly for positive bias around  $V \approx .5 \text{ eV}$ , then rises rapidly to its maximum value. This is because the bias makes the Schottky barrier smaller until it disappears completely; the potential becomes a step and the velocity mismatch becomes the important factor. Hence, the high positive bias regime is similar to the low barrier regime in Fig. 4(b). As the bias increases further, the reflection difference decreases, due to the concomitant increase in electron energy in the ferromagnet, so that the exchange splitting  $\Delta$  becomes less effective.

These results suggest that a bias could be used to control the sign and magnitude of the spin polarization.

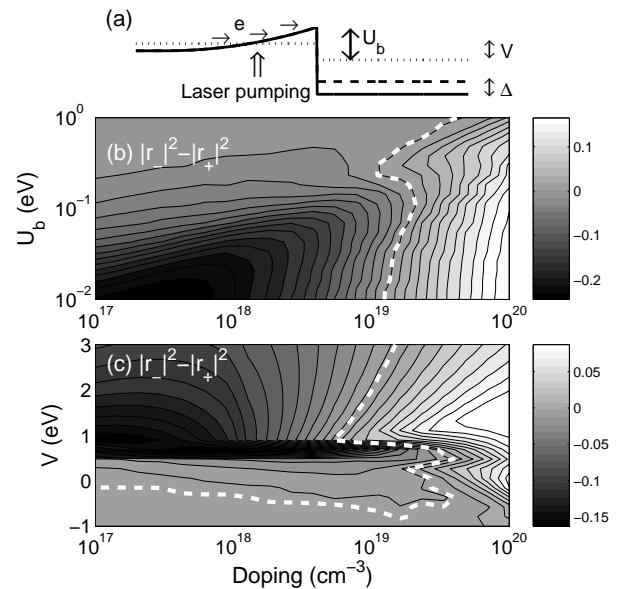


FIG. 7: Reflection from the Schottky barrier under optical excitation. (a) The band diagram. Electrons are taken to be excited homogeneously in space, including in the depletion region. (b) The spin reflection asymmetry as a function of semiconductor doping  $n$  and Schottky barrier height  $U_b$ , keeping the applied bias at  $V = 0$ . (c) The spin reflection asymmetry as a function of semiconductor doping  $n$  and applied bias  $V$ , keeping the Schottky barrier height fixed at  $U_b = 0.7 \text{ eV}$ .

For a fixed doping, the reflected spin polarization can be tuned depending on the applied bias. However, it is much easier to get high polarization for one sign of polarization than the other (in Fig. 6(b), the polarization is maximum above the change of sign, but is very nearly zero below the change of sign for low doping).

### C. Special effects of optical excitation

Optical pumping creates special effects in spin reflection at a Schottky barrier not seen under electrical injection. In the latter case, non-equilibrium electrons are injected close to the Fermi level far from the barrier whereas optical excitation creates electrons everywhere in the semiconductor, including in the space charge region. This has a profound effect on the net spin polarization because not all electrons will see the same effective barrier height. Electrons very near the interface will see a much smaller Schottky barrier than electrons pumped far away from the interface. Since the electrons closest to the interface see a smaller and narrower barrier, they will couple to the ferromagnet much more efficiently, so that the polarization is dominated by these electrons. This effect is quantitatively very important because of the exponential dependence of the tunnelling coupling on the barrier height and width. The results of optical excitation are averaged over the different barrier heights.

To fully grasp the difference between optical and electrical excitation, we attempt to quantify the optical effect. First, we assume that the electrons are pumped homogeneously in the space charge region (no contribution from the bulk region is included). In the experiment,<sup>18</sup> the semiconductor is thin enough for this to be approximately correct. The laser bandwidth is taken to be approximately 10 meV (the typical bandwidth of a pulsed laser in time-resolved pump-probe experiments). We calculate the reflection for a Gaussian distribution of electron energies for each coarse-grained spatial neighborhood in the space charge region. We then average these effects over the different barrier heights due to the homogeneous pumping along the space charge region (see Fig. 7(a)).

Results for the spin reflection difference  $|r_-|^2 - |r_+|^2$  from unpolarized excitation are shown in Fig. 7(b) as a function of doping and Schottky barrier height keeping the bias at  $V = 0$ . Compare the plot with the case of excitation at the Fermi level, Fig. 4(b). There is not much change for the low barrier region because the electrons pumped high in the barrier do not see a drastically different barrier from the electrons pumped farther away. On the other hand, at high barrier heights, there are drastic changes. The change of sign of the polarization disappears for low doping concentrations. In the case of electrical excitation, at a high barrier all the electrons see a very high and thick barrier which allows for very little tunnelling. In the case of optical pumping, there are some electrons pumped high in the barrier which see a very small barrier and are efficiently coupled to the ferromagnet. The polarization at low barrier is of opposite sign to the polarization at high barrier, but, since the coupling for low barrier is so much more efficient, it dominates and the change of sign disappears.

Figure 7(c) shows the spin reflection difference at a constant Schottky barrier height,  $U_b = 0.7$  eV, and varying doping and applied bias. In comparison with Fig. 6(b), the optical excitation drastically changes the qualitative aspects of the spin reflection difference. For low doping, the change of sign as a function of bias has been pushed down to negative bias for the same reason as the disappearance of the change of sign in Fig. 7(b) for low doping. The spin reflection difference is dominated by the electrons pumped high in the barrier, which have the opposite sign of polarization compared with the electrons near the Fermi level in the semiconductor.

There is a caveat to these special effects. A more realistic model would use an electron wavepacket to reflect off the interface in order to account for the significant scattering due to efficient optical phonon emission. The electrons pumped high in the barrier would be in a region with almost no background electron density, so that the spin lifetime may be shorter than the lifetime outside the depletion region. Our purpose here is to point out that electrical and optical experiments can give inconsistent results if it is assumed that the underlying mechanism is exactly the same in both cases. Electrically excited electrons stay close to the Fermi level, while optically ex-

cited electrons exist all over the barrier. The pumping in the barrier drastically alters the spin reflection difference which would be observed in experiments on the interface, and hence care must be taken when comparing optically excitation experiments with electrical injection experiments. In particular, the optically excited electrons pumped high in the barrier can have different sign of polarization to electrons lower in the barrier, making it difficult to compare polarizations from experiments involving optical versus electrical injection.

## V. CONCLUSIONS

We have examined the electronic properties associated with semiconductor electrons that are in proximity with a ferromagnet. Instead of focusing on the injection of ferromagnet electrons into the semiconductor through the interface, we have instead chosen to look at the properties of semiconductor electrons that can interact with a ferromagnetic epilayer. We have focused on the reflection of non-equilibrium electrons from the interface.

For doped semiconductors with ferromagnetic epilayers, we have calculated the spin-dependent reflectivities for electrons incident on the Schottky barrier from the semiconductor. We find that the shape of the barrier has a large impact on the asymmetry between reflection for the two spin channels, and significantly that the sign of the difference can change depending on the system parameters. We have included calculations that mimic the behavior of optical excitation, which can radically affect the spin reflection difference. The ability to control the sign and magnitude of the spin polarization by tuning the properties of the Schottky barrier (through the semiconductor doping or through an applied bias, for example) may be useful for device design.

In contrast to spin injection from a ferromagnet into a semiconductor, spin reflection has the advantage that the processes are kept in the semiconductor. For carriers confined near the interface, multiple reflections from the interface can enhance the single-reflection spin asymmetry, yielding larger polarizations. Such reasoning has led us to propose a spin-valve device with ferromagnetic gates.<sup>30</sup> A detailed study of the coupling of the equilibrium and transport properties of a confined semiconductor electron system in contact with the ferromagnet will be the subject of another long paper.

## Acknowledgments

This work is supported by DARPA/ONR N0014-99-1-1096, NSF DMR 0099572, the Swiss National Foundation (for CC), and University of California Campus-Laboratories Cooperation project (for JPM). We thank D.D. Awschalom, R.J. Epstein and R. Kawakami for helpful discussions.



- 
- <sup>1</sup> S. A. Wolf, D. D. Awschalom, R. A. Buhrman, J. M. Daughton, S. von Molnar, M. L. Roukes, A. Y. Chtchelkanova, D. M. Treger, *Science* **294**, 1488 (2001).
- <sup>2</sup> S. Datta and B. Das, *Appl. Phys. Lett.* **56**, 665 (1990).
- <sup>3</sup> Y. A. Bychkov and E. I. Rashba, *Sov. Phys. JETP Lett.* **39**, 78 (1984).
- <sup>4</sup> R. Fiederling, M. Keim, G. Reuscher, W. Ossau, G. Schmidt, A. Waag, L. W. Molenkamp, *Nature* **402**, 787 (1999)
- <sup>5</sup> Y. Ohno, D. K. Young, B. Beschoten, F. Matsukura, H. Ohno, D. D. Awschalom, *Nature* **402**, 790 (1999)
- <sup>6</sup> H. J. Zhu, M. Ramsteiner, H. Kostial, M. Wassermeier, H.-P. Schonherr, K. H. Ploog, *Phys. Rev. Lett.* **87**, 016601 (2001)
- <sup>7</sup> A. T. Hanbicki, B. T. Jonker, G. Itskos, G. Kioseoglou, A. Petrou, *Appl. Phys. Lett.* **80**, 1240 (2002)
- <sup>8</sup> E. Johnston-Halperin, D. Lofgreen, R. K. Kawakami, D. K. Young, L. Coldren, A. C. Gossard, D. D. Awschalom, *Phys. Rev. B* **65**, 041306 (2002)
- <sup>9</sup> J. Nitta, T. Akazaki, H. Takayanagi, T. Enoki, *Phys. Rev. Lett.* **78**, 1335 (1997).
- <sup>10</sup> U. Zülicke and C. Schroll, *Phys. Rev. Lett.* **88**, 029701 (2002).
- <sup>11</sup> D.D. Awschalom, J.M. Kikkawa, *Physics Today* **52**, 33 (1999).
- <sup>12</sup> J.M. Kikkawa, D.D. Awschalom, *Phys. Rev. Lett.* **80**, 4313 (1998).
- <sup>13</sup> J.M. Kikkawa, D.D. Awschalom, *Nature* **397**, 139 (1999).
- <sup>14</sup> I. Malajovich, J.M. Kikkawa, D.D. Awschalom, J.J. Berry and N. Samarth, *Phys. Rev. Lett.* **84**, 1015 (2000).
- <sup>15</sup> G. Salis, D. T. Fuchs, J. M. Kikkawa, D. D. Awschalom, Y. Ohno, and H. Ohno, *Phys. Rev. Lett.* **86**, 2677 (2001).
- <sup>16</sup> F. Meier, B.P. Zakharchenya, Eds., *Optical Orientation* (North-Holland, New York, 1984) and references therein.
- <sup>17</sup> R. K. Kawakami, Y. Kato, M. Hanson, I. Malajovich, J. M. Stephens, E. Johnston-Halperin, G. Salis, A. C. Gossard, D. D. Awschalom, *Science* **294**, 131 (2001).
- <sup>18</sup> R.J. Epstein, I. Malajovich, R. K. Kawakami, Y. Chye, M. Hanson, P. M. Petroff, A. C. Gossard, and D. D. Awschalom, *Phys. Rev. B* **65**, 121202 (2002).
- <sup>19</sup> C. Ciuti, J. P. McGuire, and L. J. Sham, *Phys. Rev. Lett.* **89**, 156601 (2002).
- <sup>20</sup> R.J. Epstein and D.D. Awschalom, private communication.
- <sup>21</sup> N.F. Mott and H.S.W. Massey, *The theory of atomic collisions*, third edition (Oxford University Press, London, 1965), Chapter X.
- <sup>22</sup> T. Uenoyama and L.J. Sham, *Phys. Rev. Lett.* **64**, 3070 (1990).
- <sup>23</sup> G.L. Bir, A.G. Aronov, and G.E. Pikus, *Sov. Phys. – JETP* **42**, 705.
- <sup>24</sup> J. C. Slonczewski, *Phys. Rev. B* **39**, 6995 (1989).
- <sup>25</sup> R. Monnier, M.M. Steiner, and L.J. Sham, *Phys. Rev. B* **44**, 13678 (1991).
- <sup>26</sup> G.T. Einevoll and L.J. Sham, *Phys. Rev. B* **49**, 10533 (1994).
- <sup>27</sup> J. C. Slonczewski, *J. Magn. Magn. Mater.* **195**, L1 261 (1996).
- <sup>28</sup> J. A. Katine, F. J. Albert, R. A. Buhrman, E. B. Myers, D. C. Ralph, *Phys. Rev. Lett.* **84**, 3149 (2000).
- <sup>29</sup> Y. X. Liu, D. Z.-Y. Ting, and T. C. McGill, *Phys. Rev. B* **54**, 5675 (1996).
- <sup>30</sup> C. Ciuti, J. P. McGuire, and L. J. Sham, *Appl. Phys. Lett.* **81**, 4781 (2002).